Desalination and Water Treatment
www.deswater.com
doi: 10.1080/19443994.2014.903862

54 (2015) 2648–2657
May

NOM removal by a Vacuum-UV/UV/TiO_2 reactor assisted by electron scavengers

Kamal Azrague[a,b,*], Stein W. Østerhus[a]

[a]*Department of Hydraulic and Environmental Engineering, Norwegian University of Science and Technology (NTNU), S.P. Andersensvei 5, Trondheim N-7491, Norway, Tel. +47 73 59 24 19; Fax: +47 73 59 23 76; email: kamal.azrague@sintef.no*
[b]*SINTEF Building and Infrastructure, Water and Environment, Klæbuveien 153, Trondheim 7465, Norway*

Received 16 January 2013; Accepted 9 March 2014

ABSTRACT

This paper investigates the photochemical degradation of natural organic matter (NOM) which impacts the production of drinking water. Two types of reactors (with or without immobilised TiO_2) and two types of 15 W low pressure mercury lamps (one emitting only at 254 nm and the other emitting at both 254 and 185 nm) were used. After 150 min of treatment of NOM-containing waters, the achieved average removals were 77% for the UV-absorbance at 254 nm (UV_{254}), 83% for the colour and 70% for the dissolved organic carbon. Regardless of the initial concentration, the colour increased until it reached a maximum value before decreasing. It is believed that during degradation, aromatic components of the NOM structure are transformed into intermediates which have much higher absorbance at 410 nm than their parent compounds. The investigation of the effect of various electron scavengers (oxygen (O_2), hydrogen peroxide (H_2O_2) and peroxodisulphate ($S_2O_8^{2-}$)) has shown that $S_2O_8^{2-}$ could increase the degradation rate by a factor 4 compared to the experiment without addition of any electron scavenger, while it was only 2 and 3 for O_2 and H_2O_2, respectively. However, the use of $S_2O_8^{2-}$ is limited by its cost and sulphate ion residual.

Keywords: Advanced oxidation; Electron scavenger; Natural organic matter; Peroxodisulphate; Photocatalysis; Vacuum UV

1. Introduction

Natural organic matter (NOM) occurs in all natural water sources when animal and plant materials break down. The main terrestrial NOM component is attributed to humic substances. Humic substances can be divided into three groups depending on the method of isolation from the original substance. These are fulvic acid, humic acid and humin [1]. The mechanism of formation of humic substances and their structures are not well described but they are known to contain high carbon content (50–60%) of both aliphatic and aromatic character and to be rich in oxygen-containing functionalities [2].

Humic substances represent a serious issue for the drinking water production for several reasons. They impart a brown/yellow colour to water [3,4], they can complex with metals [5,6] and organic pollutants, such as pesticides [7]. Moreover, they diminish the removal of other contaminants, they foul membranes, they can reduce the disinfection efficiency, and finally they are the precursors of mutagenic halogenated compounds

---

*Corresponding author.

in water formed after chlorination (disinfection by-products) [8,9]. In addition, recent data have shown significant increase in NOM concentration and reactivity across Scandinavia [3,4] and Germany. However, it is in the UK that the largest proportional increase has occurred [3,10]. Indeed, this observation could be attributed to climate change which certainly might affect the treatment strategy to produce drinking water from surface water [3].

Among methods for NOM removal, the most used for practical and economical reasons is coagulation/flocculation. This method is effective at removing NOM but only the large molecular weight hydrophobic fraction of it, leaving the hydrophilic fraction behind. Hence, the water treatment facilities need to invest in additional NOM removal methods where the existing water treatment process becomes inadequate. Recently, there is a growing interest on the evaluation of the use of advanced oxidation processes (AOP) to mineralise NOM and other micropollutants. AOPs generate hydroxyl radicals ($HO^\bullet$) which are the second strongest oxidant after fluorine and are able to oxidise and mineralise almost every organic molecule, yielding CO_2 and inorganic ions. The UV/TiO_2 photocatalytic process is among the most studied AOP. Literature reports that it effectively treats NOM with up to 80% removal of TOC and 98% of colour. However, if an insufficient treatment time is used, easily biodegradable organic matter may remain in the solution [11,12] that would require a subsequent biological treatment. Vacuum ultra-violet (V-UV) lamps can be used for water [13] and air treatments [14]. By producing a large amount of $HO^\bullet$ via the photolysis of water, such lamps have a considerable potential for application [15]. Combining V-UV and photocatalysis has shown to be very efficient [16].

In this work, we have used a commercial unit with immobilised TiO_2 (to avoid a separation step) irradiated with a low pressure mercury lamp emitting at two wavelengths 254 and 185 nm for the treatment of NOM-containing water. To evaluate each process within the commercial unit, a copy of the photoreactor without immobilised TiO_2 and another lamp emitting only at 254 nm have also been used. In addition, in order to improve the oxidation, the effects of oxygen, hydrogen peroxide and peroxodisulphate have been investigated.

2. Materials and methods

2.1. Chemicals

All the chemicals for these experiments were of laboratory reagent quality. Hydrogen peroxide (35% (v/v)), Phosphoric acid (85% (v/v)), potassium peroxodisulphate, hydrochloric acid and sodium hydroxide were purchased from Merck. The NOM concentrate used is a regeneration solution from an anion exchanger for NOM removal at a drinking water treatment plant in Meråker, Norway. Fractionation following the method described in [3], was used to determine the concentrations of four NOM fractions: very hydrophobic acids (VHA), slightly hydrophobic acids (SHA), charge hydrophilics (CHA) and neutral hydrophilics (NEU). The results showed that the VHA fraction was the dominant fraction (64%) followed by the SHA fraction with 16%, then the CHA fraction with 11% and the NEU fraction with 9%. Further comparison of the raw water used in this study with natural water, obtained from a lake near Trondheim, Norway, showed no significant differences. Indeed, for this natural water, VHA fraction was also the dominant fraction (71%), followed by the SHA fraction with 14%, then the NEU with 10% and the CHA fraction with 5%.

2.2. Experimental set-up

Experiments were conducted in batch mode using an annular reactor (M300 water purifier®) provided by Wallenius Water AB. The photoreactor was 330 mm high, with an inner diameter of 44 mm and the lamp was placed in the centre of the photoreactor with a quartz tube protection (diameter 22 mm). In order to investigate the importance of each process involved (namely photolysis, photocatalysis and V-UV photolysis of water) during the degradation of NOM by this system, different configurations were used. As previously mentioned, two types of reactors (with or without immobilised TiO_2) and two types of 15 W low pressure mercury lamps (one emitting only at 254 nm and the other emitting at both 254 and 185 nm) were used. The two lamps had an approximate photon flux of $(1.2 \pm 0.1) \times 10^{-5}\,\mathrm{mol\,s^{-1}}$ at 254 nm. The available water volume of the photoreactor was 0.34 L and the total volume of the batch was 10 L. Gases (N_2, air or O_2) were added at a flow of $250\,\mathrm{mL\,min^{-1}}$ before the inlet of the photoreactor. A schematic sketch of the reactor and the complete system set-up is shown in Fig. 1.

The solution was continuously re-circulated through the photoreactor using a pump at a flow rate of $800\,\mathrm{L\,h^{-1}}$ corresponding to a turbulent flow regime ($Re \sim 18{,}000$), which allowed an efficient transport of NOM towards the oxidation sites. The temperature of the solution was maintained at 20°C.

2.3. Preparation of NOM solutions

The water solutions used in this study were prepared by mixing distilled water and the NOM concentrate (Origin provided in section 2.1). Before mixing with water, the concentrate was acidified to

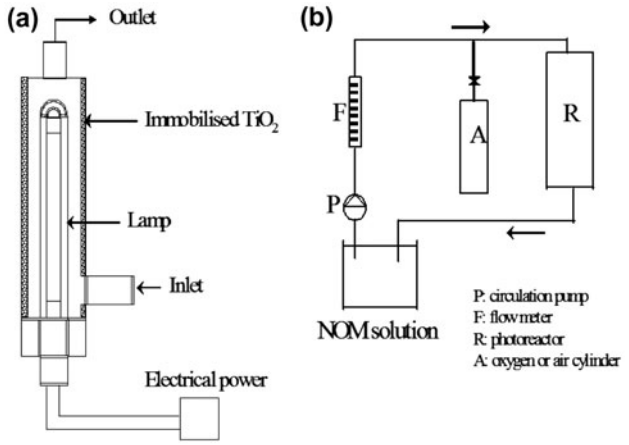

Fig. 1. (a) Schematic sketch of the annular V-UV/UV/TiO_2 reactor. When using the UV or the V-UV system with or without TiO_2. (b) Experimental set-up.

pH 7 (by adding HCl) in order to reduce the carbonate to an acceptable level by stripping off the CO_2. The characteristics of the resulting water quality were as follows: Colour: 50 mg Pt L^{-1}; Conductivity: 590 µS cm^{-1}; DOC: 6.3 mg L^{-1}; and UV_{254}: 0.37 cm^{-1}. The resulting alkalinity was between 0.3 and 1 mM depending on the amount of added sodium bicarbonate.

2.4. *Addition of hydrogen peroxide and potassium peroxodisulphate*

2.4.1. *Hydrogen peroxide (H_2O_2)*

Various amounts of H_2O_2 (35% v/v) were used to have an initial concentration varying from 0.25 to 1.5 mmol L^{-1}. The H_2O_2 was directly added to 10 L of NOM-containing water.

2.4.2. *Potassium peroxodisulphate ($K_2S_2O_8$)*

A stock solution consisting of 3 g of $K_2S_2O_8$ dissolved in 1 L distilled water was prepared. The stock solution was then diluted by 1/10 (v/v) with NOM-containing water to give a total volume of 10 L with a final concentration of 300 mg L^{-1} (or 1.1 mmol L^{-1}) for the $K_2S_2O_8$ and the correct NOM content (Colour 50 mg Pt L^{-1} and DOC = 6.3 mg L^{-1}). Peroxodisulphate is not commonly used for the drinking water treatment but commonly employed for the treatment of fluids in the petroleum industry [17] for the treatment of hazardous wastewater [18–20] and as reaction initiator [17]. The peroxodisulphate ($S_2O_8^{2-}$, $E^o = 2.01$ V) is a strong oxidant that can be activated to generate an even stronger oxidant known as a sulphate radical ($SO_8^{-\bullet}$, $E^o = 2.4$ V) [21].

2.5. *Analyses*

Samples were taken from the feed tank during irradiation and filtered through 0.45 µm Millipore membrane filters. Alkalinity and pH were analysed using Metrohm Titroprocessor 726 equipped with sample changer 717 and Dosimat 685. Dissolved organic carbon (DOC) was analysed using a carbon analyser Tekmar Dohrmann Apollo 9,000 total organic. Prior to the DOC analysis, pH was adjusted to 2 using phosphoric acid. Turbidity was measured using a HACH 2100 N turbidimeter. Colour (which is the number representing the platinum concentration—mg Pt L^{-1}—in a platinum cobalt chloride solution that has the same absorbance at 410 nm as the sample) and UV_{254} (which is the absorbance at the wavelength 254 nm) were measured using a Hitachi U-3000 Spectrophotometer. Prior to UV_{254} and colour measurements, the samples were adjusted to pH 7 using HCl and NaOH.

3. Reaction mechanisms

In one of the experimental configurations, the unit used combines a lamp emitting at 185 and 254 nm and a reactor with immobilised TiO_2 on the internal surface. Under such experimental conditions, three different processes can take place in the reactor and degrade the organic compounds contained in the water: UV photolysis and two AOPs: TiO_2 photocatalysis and V-UV water photolysis. One may also envisage that ozone could be formed from oxygen absorbing V-UV irradiations. However, due to low dissolved oxygen concentration in water and its weak absorption coefficient at 185 nm (about 0.1 cm^{-1} atm^{-1} in the gas phase [22]) compared to the much larger water concentration and extinction coefficient at 185 nm (1.8 cm^{-1}) [23], the production of ozone is not believed to occur in the aqueous phase.

3.1. *Direct UV photolysis*

NOM are conjugated olefinic, aromatic, phenolic-semiquinone-quinone structures containing macromolecules of humic acid with a wide spectrum of functional groups (−C=O, −COOH, −OH, −NH−, −N=) and chromophores that are capable of absorbing electromagnetic radiations [24]. Consequently and according to the UV–visible spectrum of the NOM solution, (Fig. 2, $t = 0$ min) a direct photolysis of NOM by the irradiation at 254 nm could occur.

3.2. V-UV photolysis of water

Since the 185 nm irradiation is situated in the V-UV, the photolysis of water occurs and leads to the formation of hydroxyl radicals with a quantum yield of 0.33 (Eq. (1)) [25]. In turn, generated $HO^{\bullet}$ oxidises the NOM.

$$H_2O + hv\,(V - UV) \rightarrow HO^{\bullet} + H^{\bullet} \tag{1}$$

3.3. UV/TiO$_2$ photocatalysis

During excitation, the energy is transferred to the semiconductor (TiO_2) through UV irradiations with sufficient energy ($\lambda \leq 380$ nm) and electrons are excited and leave the valence band (VB) for the conduction band (CB) leading to the creation of positive holes (h^+) in VB and a liberation of electrons (e^-) in the CB (Eq. (2)). On the TiO_2 surface, the holes (h^+) react with H_2O or OH^- engendering hydroxyl radicals ($HO^{\bullet}$) (Eqs. (3) and (4)). At the same time, electrons transferred into the CB, can react with oxygen and form superoxide anions ($O_2^{\bullet -}$) (Eq. (5)). The superoxide ion can further react with water giving additional hydroxyl radicals, hydroxide ions and oxides (Eqs. (6) and (7)). OH^- from the latest reaction can react with the holes in the VB generating even more hydroxyl radicals (Eq. (4)). The hydroxyl radicals with their strong oxidising capacity together with the oxidising capacity of the positive holes gives powerful oxidation of the organic compounds adsorbed to the TiO_2 surface [26].

$$TiO_2 + hv(\lambda \leqslant 380\,\text{nm}) \rightarrow h^{+}{}_{(VB)} + e^{-}{}_{(CB)} \tag{2}$$

$$h^+ + H_2O \rightarrow HO^{\bullet} + H^+ \tag{3}$$

$$h^+ + OH^- \rightarrow HO^{\bullet} \tag{4}$$

$$e^- + O_2 \rightarrow O_2{}^{\bullet -} \tag{5}$$

$$2O_2{}^{\bullet -} + 2H_2O \rightarrow H_2O_2 + 2\,OH^- + O_2 \tag{6}$$

$$H_2O_2 + e^- \rightarrow OH^- + HO^{\bullet} \tag{7}$$

4. Results and discussion

4.1. Degradation of NOM by the V-UV/UV/TiO$_2$ reactor

4.1.1. UV$_{254}$, colour and DOC removal

The changes in the absorption spectrum of the NOM during the photodegradation process at different irradiation times are shown in Fig. 2. The spectrum of NOM in the UV–visible region displays a superposition of absorption bands corresponding to a composite local-excitation band, a composite benzenoid band and a composite electron-transfer band, as reported in the literature [27]. During the irradiation, the decrease of absorption peaks (Fig. 2) indicates a rapid transformation or degradation of the NOM chromophores.

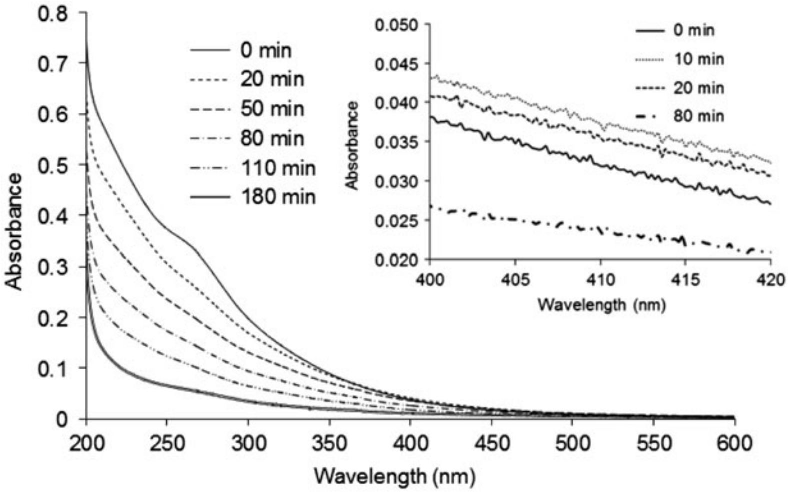

Fig. 2. UV–visible spectrum of the NOM solution at different irradiation times using the (UV/V-UV/TiO_2) system, (pH 7; Colour 50 mg Pt L^{-1}; and DOC = 6.3 mg L^{-1}).

The changes in UV_{254}, colour and DOC have been monitored during the degradation, and the results are shown in Fig. 3. DOC was less frequently analysed, for the reason that a large reaction volume is required per analysis. According to UV_{254} and colour measurements, the degradation of the NOM appeared to be near completion after 150 min, with reduction of 77 and 83%, respectively. However, DOC analysis suggested that mineralisation is lower, reaching 70% removal. These results indicate that significant chemical changes have occurred in the NOM structures via oxidation due to $HO^\bullet$ or photo transformation since the conjugated bonds (including unsaturated aldehydes and aromatics) absorb at 254 nm. In contrary to absorbance at 254 nm, colour does not follow a first-order kinetic but a more complex kinetic. Regardless of the initial concentration, the development of the colour (Fig. 3) and the absorbance in the region of 400 nm (Fig. 2) show an increase until it reaches a maximum value before decreasing. To our knowledge, this phenomenon has not been reported in the literature. It is believed that, during the degradation of some aromatic compounds within the NOM structure, there is a production of intermediates which have a much higher absorbance at 410 nm than the parent compounds. Further research will be carried out to investigate the intermediates formed and to bring answers to this phenomenon.

DOC was reduced at a rate slower than the reduction of both UV_{254} and colour, reaching a removal of approximately 70% after 150 min, which confirms that the NOM is not degraded directly to carbon dioxide and water but via various reactions leading to the formation of many intermediates having different removal rates and contributing to the DOC level and to the UV–visible absorbance. Indeed, it is well known that oxidation and photolysis break down large molecules into smaller intermediates which are characterized as low molecular acids and neutral compounds [28,29].

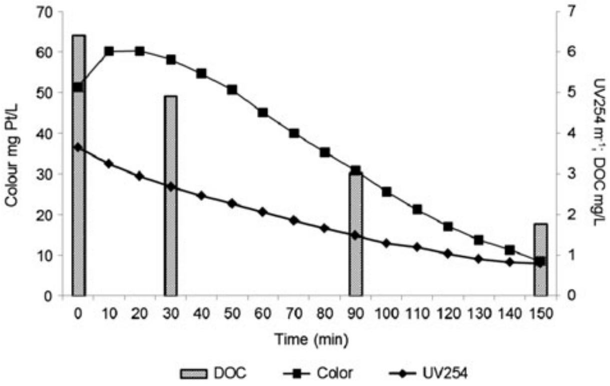

Fig. 3. Changes in colour, UV_{254} and DOC of NOM-containing water during irradiation using the (UV/V-UV/TiO_2) system, (pH 7; Colour 50 mg Pt L^{-1}; and DOC = 6.3 mg L^{-1}).

4.1.2. Kinetic study

In general, the photocatalytic degradation can be well described by the Langmuir–Hinshelwood kinetic model, in which the reaction rate (r) varies proportionally with the surface coverage (θ) and is a function of the concentration C [26]:

$$r = \frac{dC}{dt} = k_r\theta = \frac{k_rKC}{1+KC} \tag{8}$$

where C is the concentration of pollutant (mol L^{-1}), t is the irradiated time (s), k_r is the Langmuir–Hinshelwood photocatalytic rate constant (mol L^{-1} s^{-1}) and K is the adsorption constant (L mol^{-1}). However, according to [26] at low concentration ($C < 10^{-3}$ M), the product KC is negligible with respect to unity, leading to Eq. (9) which describes the first-order kinetics as follows:

$$r = k_rKC = k_{\text{Photocatalyse}}C \tag{9}$$

The absorbance at 254 nm has been used as a measure to assess the kinetics and establish the efficiency of the different processes involved.

Results in Fig. 4 obtained using different configurations (without addition of gas), show that the two other processes (photolysis and V-UV) follow also a pseudo-first-order kinetic. Consequently, when the complete process (V-UV/UV/TiO_2) is used for the removal of the UV_{254}, a pseudo-first-order reaction kinetic can be employed:

$$\begin{aligned} r = \frac{d\text{UV}_{254}}{dt} &= -(k_{\text{Photocatalyse}} + k_{\text{Photolyse}} + k_{\text{V-UV}})\text{UV}_{254} \\ &= -k_{\text{app}}\text{UV}_{254} \end{aligned} \tag{10}$$

Thus, the development of the UV_{254} is modelled by the Eq. (11):

$$(\text{UV}_{254})_t = (\text{UV}_{254})_0\, e^{-k_{\text{app}}.t} \tag{11}$$

All the degradations have been found to be well modelled by the pseudo-first-order kinetic (Fig. 4) and the rate constants are reported in Table 1.

It is obvious that the most efficient process for NOM removal in this unit is the V-UV process which

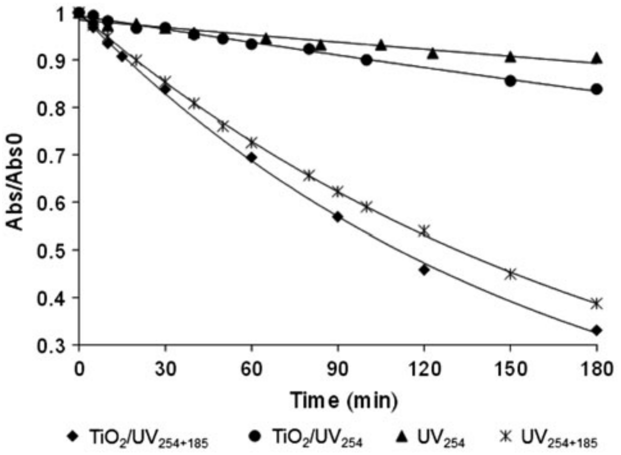

Fig. 4. Normalised experimental and calculated (—) absorbance at 254 nm for NOM in the feed tank vs. irradiation time using different reactor configurations (pH 7; Colour 50 mg Pt L^{-1}; and DOC = 6.3 mg L^{-1}). Calculated absorbance vs. time was determined using Eq. (11).

represents 76% of the total removal efficiency at a given time. The photolysis and photocatalysis contribute considerably less to the NOM degradation than the V-UV process. However, generated $HO^{\bullet}$ from V-UV is only able to oxidise NOM in a layer close to the quartz sleeves of the lamp. Indeed, 99% of the irradiation at 185 nm is absorbed in 10 mm thickness due to the high absorptivity of water at 185 nm (3.2 cm^{-1}) [23].

4.2. Effect of pH

The results in the Fig. 5 show that the rate of degradation is increasing with the pH and this phenomenon could be explained as follows:

- A majority of acidic groups will be ionised above pH 4 and a majority of phenolic groups will only be ionised above pH 9 [30]. This ionisation will lead to a negative charge on the humic acid molecules and consequently to repulsions, engendering linear humic acids [30–32]. This linear conformation offers the oxidants better accessibility to the double bonds than in coiled molecules at lower pHs [33–35].
- Another contributing effect is the higher concentration of hydroxyl anions at higher pH giving increased generation of hydroxyl radicals (Eqs. (4) and (12)) [30].

$$OH^{-} + h\nu(185\ \text{nm}) \rightarrow OH^{\bullet} + e^{-}_{(\text{solvated})}) \tag{12}$$

4.3. Effect of carbonates

Carbonate and bicarbonate ions are known to be radical scavengers, and since $CO_3^{\bullet-}$ (1.78 V/ENH) is much less reactive than $HO^{\bullet}$ (2.8 V/ENH), inhibition by carbonate ions influences the degradation. Results in Fig. 5 illustrate that the effect of added sodium bicarbonate is more pronounced at pH 10 than at pH 7 and 5. This is caused by the relative distribution of carbonate species, and the fact that CO_3^{2-} is a more efficient $HO^{\bullet}$ scavenger than HCO_3^{-}. According to some authors [36,37], carbonate ion has a more

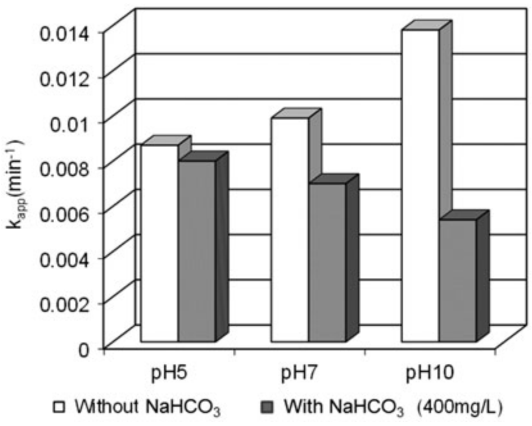

Fig. 5. The effect of pH and carbonates on the apparent photodegradation rate constants of NOM using the (UV/V-UV/TiO_2) system (Lamp 185 + 254) and (Colour 50 mg Pt L^{-1}). Calculated k_{app} was determined using Eq. (11).

Table 1
Pseudo-first-order rate constants for the different reactor configurations

	UV_{254} (Photolysis)	$UV_{185+254}$ (Photolysis + V-UV)	UV_{254}-TiO_2 (Photolysis + Photocatalysis)	$UV_{185–254}$-TiO_2 (Photolysis + Photocatalysis + V-UV)
k_{app}	5.4×10^{-4} min^{-1}	5.3×10^{-3} min^{-1}	9.7×10^{-4} min^{-1}	6.2×10^{-3} min^{-1}

important effect than bicarbonate ion which is illustrated by reaction rates for Eqs. (13) and (14).

$$HCO_3^- + {}^{\bullet}OH \rightarrow CO_3^{-\bullet} + H_2O \quad k_1 = 8.5 \times 10^6\,M^{-1}\,s^{-1} \tag{13}$$

$$CO_3^{2-} + {}^{\bullet}OH \rightarrow CO_3^{-\bullet} + OH^- \quad k_2 = 3.8 \times 10^8\,M^{-1}\,s^{-1} \tag{14}$$

Hence, the presence of carbonate species in the water can result in a significant reduction in the removal efficiency of NOM. In order to avoid such reductions, the pH in waters highly carbonated should be as low as possible to convert carbonate and bicarbonate to bicarbonate and carbonic acid, respectively. However, in less-carbonated water a higher pH is recommended.

4.4. *Effect of added electron scavengers*

During the operation of the V-UV/UV/TiO_2 reactor, electrons are transferred to the conduction band (Eq. (2)) and solvated in water (Eqs. (15, 16)).

$$H_2O + h\nu(<200\text{ nm}) \rightarrow [e^-, H_2O^+] + (H_2O) \tag{15}$$

$$[e^-, H_2O^+] + (H_2O) \rightarrow e^-_{aq} + HO^{\bullet} + H_3O^+ \tag{16}$$

Therefore, a recombination of electrons with positive holes (Eq. (17)) and with hydroxyl radicals (Eq. (18)) could occur and reduce the available amount of hydroxyl radicals.

$$TiO_2\,(h^+ + e^-) \rightarrow TiO_2 \tag{17}$$

$$HO^{\bullet} + e^-_{(\text{solvated})} + H^+ \rightarrow H_2O \tag{18}$$

The only way to avoid or limit such recombination is to scavenge the electrons formed by adding a compound which is an electron acceptor. Three different electron scavengers namely O_2, H_2O_2 and $S_2O_8^{2-}$ have been evaluated for this purpose. Fig. 6 reports the obtained results with respect to UV_{254} and colour removal. The effects are discussed in the following subsections.

4.4.1. *Effect of oxygen*

The oxygen concentration is a very important parameter for both the photocatalysis process [38] and for the V-UV process [39,40]. It could play a key role in the adsorption onto TiO_2 [30], for the formation of oxidising species [13,15], and on the mineralisation of organic pollutants [38,40]. Indeed, oxygen reacts with an electron to form a superoxide anion (Eq. (5)), or with hydrogen peroxide formed *in situ* leading to $HO^{\bullet}$ (Eq. (7)). These reactions limit the recombination between the different charges (e^- with h^+ or $HO^{\bullet}$). Its effect has been assessed using three different conditions namely, addition of air (before and during the irradiation experiment), oxygen and nitrogen, allowing different oxygen concentrations in the photoreactor. Fig. 7 confirms a faster degradation with oxygen than with air or nitrogen addition. Therefore, an addition of oxygen could be considered to optimise the efficiency of such unit when treating NOM-containing waters. An even more improved oxidation could also take place if the oxygen is added directly in the reactor, as under V-UV irradiations (<200 nm) oxygen bubbles generate ozone [41], which is known to be a strong oxidant able, in turn, either to oxidise directly the NOM molecules or indirectly by generating more $HO^{\bullet}$. Ozone is not produced in the configuration tested in this study, as the oxygen is introduced in the solution prior to enter the reactor.

4.4.2. *Effect of H_2O_2*

Added H_2O_2 enhances the UV and colour removal significantly as shown in Fig. 6. The reaction kinetic obeys a first-order reaction with respect to UV_{254}. In addition to scavenging electrons (Eq. (7)), H_2O_2 is transformed into hydroxyl radicals via the same reaction (Eq. (7)) but also via the photolysis (Eq. (19)) and via attacks of hydrogen radicals (Eq. (20)).

When using an addition of hydrogen peroxide there is a large potential to optimise the use of irradiations emitted to produce hydroxyl radicals. However, the applied hydrogen peroxide dosage should be optimal to avoid a reduced degradation rate due to an excess of H_2O_2 which scavenges $HO^{\bullet}$ (Eq. (21)) [42].

$$H_2O_2 + h\nu\,(185 + 254) \rightarrow 2\,HO^{\bullet} \tag{19}$$

$$H_2O_2 + H^{\bullet} \rightarrow H_2O + HO^{\bullet} \tag{20}$$

$$H_2O_2 + HO^{\bullet} \rightarrow HO_2^{\bullet} + H_2O \tag{21}$$

Hence, different experiments using various concentrations of H_2O_2 have been carried out in order to determine the optimal dose. The results reported in the Fig. 7 show that the UV removal improves by augmenting the H_2O_2 concentration. However, from this figure the optimal concentration seems to be close to

1 mM (34 mg L^{-1}) which is within the range that is typically used in the literature. Indeed, when increasing further the dose of H_2O_2, the rate does augment but in a smaller extent. Nevertheless, the optimal dose allows an increase in the rate of a factor 2 compared to the experiment with O_2 and of a factor 3 compared to the experiment without added oxidant. The same tendency was obtained for the colour removal. Furthermore, one may note that at a low concentration, the hydrogen peroxide might limit the recombination of charges before acting as a significant additional oxidation process.

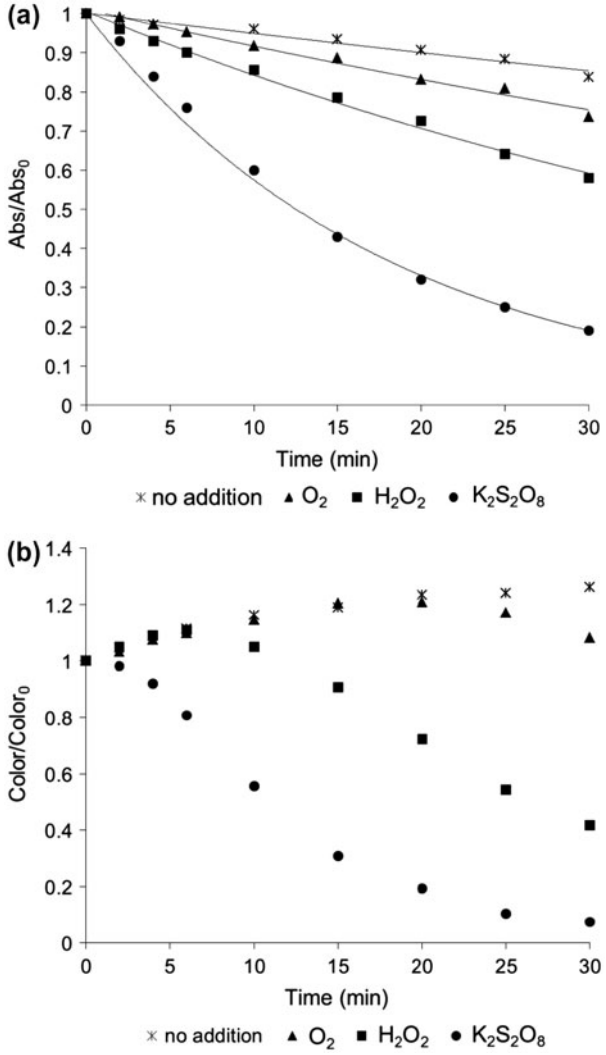

Fig. 6. The effect of addition of different electron scavengers using the (UV/V-UV/TiO_2) system (Lamp 185 + 254), ($[H_2O_2] = 1.5$ mmol L^{-1}; $[K_2S_2O_8] = 1.1$ mmol L^{-1}; $[O_2] = 0.3$ mmol L^{-1}; without gas addition; pH 7; Colour 50 mg Pt L^{-1}; and DOC = 6.3 mg L^{-1}) on the (a) UV_{254} reduction and (b) colour removal.

4.4.3. *Effect of peroxodisulphate*

Compared to the experiment free of added oxidant, the addition of $S_2O_8^{2-}$ clearly enhances the removal of UV_{254} and colour, as shown in Fig. 6. Furthermore, no increase in colour has been observed during the first stage of the treatment as was the case for other combinations (Fig. 6). The fact that electrons on the TiO_2 conduction band and solvated electrons are scavenged by the $S_2O_8^{2-}$ (Eqs.(22–24)), avoiding e^-/h^+ or $e^-/HO^\bullet$ recombination, may explain the faster removals. Nevertheless, one may note that photolysis of $S_2O_8^{2-}$ also produces two sulphate radical anions (Eq. (23)) which are also strongly oxidising species ($E^o = 2.6$ V) that are able to oxidise directly the NOM or via the generation of hydroxyl radicals (Eq. (24)).

$$e^- + S_2O_8^{2-} \rightarrow SO_4^{2-} + SO_4^{\bullet -} \tag{22}$$

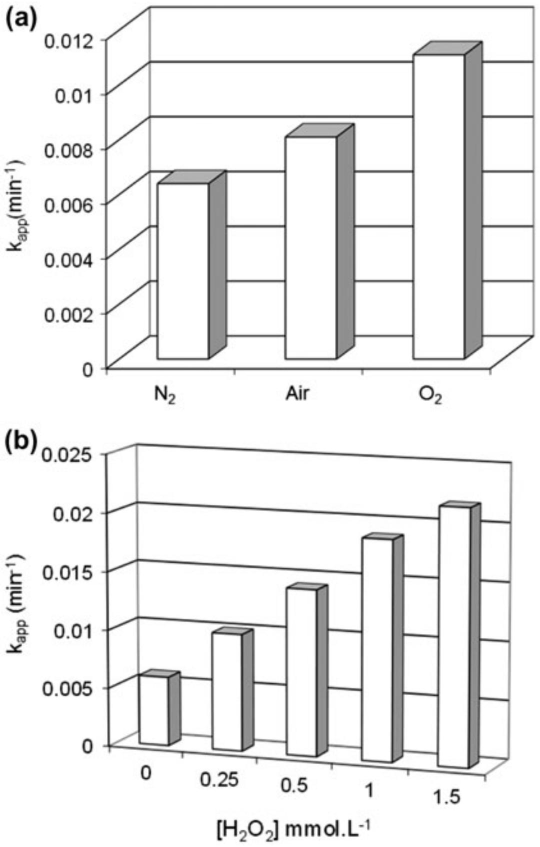

Fig. 7. The effect of different O_2 levels and addition of hydrogen peroxide at different concentrations on the apparent rate constant of photodegradation of NOM using the full system (UV/V-UV/TiO_2) system (Lamp 185 + 254), (pH 7; Colour 50 mg Pt L^{-1}; and DOC = 6.3 mg L^{-1}). Calculated k_{app} was determined using Eq. (11).

$$S_2O_8^{2-} + hv\,(185 + 254) \rightarrow 2\,SO_4^{\bullet -} \tag{23}$$

$$SO_4^{\bullet -} + H_2O \rightarrow SO_4^{2-} + HO^{\bullet} + H^{+} \tag{24}$$

$S_2O_8^{2-}$ seems to be much more efficient than H_2O_2 for the same initial concentration of nearly 1 mM which assures being within the allowed limit of residual sulphate concentration. Indeed, although sulphate does not pose any health risk, the USEPA has listed it under the secondary drinking water standards with a maximum concentration of 250 mg/L (1.43 mmol L^{-1}) based on aesthetic reasons, such as taste and odour [43,44].

Addition of $S_2O_8^{2-}$ should, as addition of H_2O_2, be considered for potential improvement of the process. The only limiting factors are the high cost of peroxodisulphate (30–35 $/kg) compared to hydrogen peroxide (0.6–1.3 $/kg) [45], and high residual concentration of sulphate ions in the treated water [19,45].

5. Conclusion

The Vacuum-UV/UV/TiO_2 reactor (M300 water purifier unit) originally designed for ballast water treatment and disinfection, using a combination of Vacuum-UV and UV/TiO_2, has been shown to be effective for the degradation of NOM. Within this system, V-UV is the most efficient process in comparison to photocatalysis and photolysis. Addition of electron scavengers has shown to improve the efficiency of the system by limiting the recombination or by producing more $HO^{\bullet}$ via different mechanisms during the irradiation. Oxygen increased the degradation rate by a factor of 2, H_2O_2 by a factor of 3 and $S_2O_8^{2-}$ by a factor of 4 compared to the rate of the experiment without any added electron scavengers. Peroxodisulphate has been shown to be the most effective electron scavenger. However, there are two factors which could limit its use, which are the chemical costs and the residual sulphate ion concentration in treated water. Overall, based on these results, it can be concluded that such systems are not an alternative for conventional water treatments. Indeed, for the water quality used within this study (80% hydrophobic acids), enhanced coagulation remains the most suitable treatment technology. Nevertheless, these systems could be considered as a polishing step to remove remaining humic fractions and other persistent organic compounds that may be present. This is very relevant for several industrial applications, as e.g. microelectronic or pharmaceutical productions, where ultra-pure water is required.

Acknowledgements

The authors wish to thank Wallenius Water AB for supplying the photoreactor and the European project TECHNEAU for the financial support.

References

[1] J.C.A. De Wuilloud, R.G. Wuilloud, B.B.M. Sadi, J.A. Caruso, Trace humic and fulvic acid determination in natural water by cloud point extraction/preconcentration using non-ionic and cationic surfactants with FI-UV detection, Analyst 128 (2003) 453–458.

[2] Y. Cho, W. Choi, Visible light-induced reactions of humic acids on TiO_2, J. Photochem. Photobiol., A 148 (2002) 129–135.

[3] R. Fabris, C.W.K. Chow, M. Drikas, B. Eikebrokk, Comparison of NOM character in selected Australian and Norwegian drinking waters, Water Res. 42 (2008) 4188–4196.

[4] A. Matilainen, E.T. Gjessing, T. Lahtinen, L. Hed, A. Bhatnagar, M. Sillanpää, An overview of the methods used in the characterisation of natural organic matter (NOM) in relation to drinking water treatment, Chemosphere 83 (2011) 1431–1442.

[5] H.A. Al-Reasi, C.M. Wood, D.S. Smith, Physicochemical and spectroscopic properties of natural organic matter (NOM) from various sources and implications for ameliorative effects on metal toxicity to aquatic biota, Aquat. Toxicol. 103 (2011) 179–190.

[6] D. Schmitt, F. Saravia, F.H. Frimmel, W. Schuessler, NOM-facilitated transport of metal ions in aquifers: Importance of complex-dissociation kinetics and colloid formation, Water Res. 37 (2003) 3541–3550.

[7] J.F. McCarthy, Bioavailability and toxicity of metals and hydrophobic organic contaminants, in: I.H. Suffet, P. MacCarthy (Eds.), Aquatic Humic Substances: Influence on Fate and Treatment of Pollutants, American Chemical Society, Washington DC, 1989, pp. 263–279.

[8] H.C. Lin, G.S. Wang, Effects of UV/H_2O_2 on NOM fractionation and corresponding DBPs formation, Desalination 270 (2011) 221–226.

[9] P. Roccaro, F.G.A. Vagliasindi, Differential vs. absolute UV absorbance approaches in studying NOM reactivity in DBPs formation: Comparison and applicability, Water Res. 43 (2009) 744–750.

[10] B. Eikebrokk, R.D. Vogt, H. Liltved, NOM increase in Northern European source waters: Discussion of possible causes and impacts on coagulation/contact filtration processes, Water Sci. Technol. Water Supply 4 (2004) 47–52.

[11] M. Bekbolet, I. Balcioglu, Photocatalytic degradation kinetics of humic acid in aqueous TiO_2 dispersions: The influence of hydrogen peroxide and bicarbonate ion, Water Sci. Technol. 34 (1996) 73–80.

[12] M. Bekbolet, F. Cecen, G. Ozkosemen, Photocatalytic oxidation and subsequent adsorption characteristics of humic acids, Water Sci. Technol. 34 (1996) 65–72.

[13] K. Azrague, E. Bonnefille, V. Pradines, V. Pimienta, E. Oliveros, M.T. Maurette, F. Benoit-Marquié, Hydrogen peroxide evolution during V-UV photolysis of water, Photochem. Photobiol. Sci. 4 (2005) 406–408.

[14] P. Monneyron, A. De La Guardia, M.H. Manero, E. Oliveros, M.T. Maurette, F. Benoit-Marquié, Co-treatment of industrial air streams using A.O.P. and adsorption processes, Int. J. Photoenergy 5 (2003) 167–174.

[15] M.G. Gonzalez, E. Oliveros, M. Worner, A.M. Braun, Vacuum-ultraviolet photolysis of aqueous reaction systems, J. Photochem. Photobiol., C 5 (2004) 225–246.

[16] W. Han, P. Zhang, W. Zhu, J. Yin, L. Li, Photocatalysis of p-chlorobenzoic acid in aqueous solution under irradiation of 254 nm and 185 nm UV light, Water Res. 38 (2004) 4197–4203.

[17] F.I. Hai, K. Yamamoto, K. Fukushi, Hybrid treatment systems for dye wastewater, Crit. Rev. Environ. Sci. Technol. 37 (2007) 315–377.

[18] M. Hepel, J. Luo, Photoelectrochemical mineralization of textile diazo dye pollutants using nanocrystalline WO3 electrodes, Electrochim. Acta 47 (2001) 729–740.

[19] A.R. Khataee, O. Mirzajani, UV/peroxydisulfate oxidation of C. I. Basic Blue 3: Modeling of key factors by artificial neural network, Desalination 251 (2010) 64–69.

[20] T. Kurechi, M. Aizawa, A. Kunugi, Studies on the antioxidants XVIII: Oxidation product of tertiary butyl hydroquinone, JAOCS 60 (1983) 1878–1882.

[21] R.E. Huie, C.L. Clifton, P. Neta, Electron transfer reaction rates and equilibria of the carbonate and sulphate radical anions, Int. J. Radiat. Appl. Instrum. C: Radiat. Phys. Chem. 38 (1991) 477–481.

[22] J.M. Dohan, W.J. Masschelein, The photochemical generation of ozone: Present state–of–the–art, Ozone Sci. Eng. 9 (1987) 315–334.

[23] J.L. Weeks, G.M. Meaburn, S. Gordon, Absorption coefficients of liquid water and aqueous solutions in the far ultraviolet, Radiat. Res. 19 (1963) 559–567.

[24] C.S. Uyguner, M. Bekbolet, Evaluation of humic acid photocatalytic degradation by UV–vis and fluorescence spectroscopy, Catal. Today 101 (2005) 267–274.

[25] N. Getoff, G.O. Schenck, Primary products of liquid water photolysis at 1236, 1470 and, 1849 Å, Photochem. Photobiol. 8 (1968) 167–178.

[26] J.M. Herrmann, Heterogeneous photocatalysis: Fundamentals and applications to the removal of various types of aqueous pollutants, Catal. Today 53 (1999) 115–129.

[27] G.V. Korshin, C.W. Li, M.M. Benjamin, Monitoring the properties of natural organic matter through UV spectroscopy: A consistent theory, Water Res. 31 (1997) 1787–1795.

[28] S. Liu, M. Lim, R. Fabris, C. Chow, K. Chiang, M. Drikas, R. Amal, Removal of humic acid using TiO_2 photocatalytic process—Fractionation and molecular weight characterisation studies, Chemosphere 72 (2008) 263–271.

[29] S. Liu, M. Lim, R. Fabris, C.W. Chow, M. Drikas, G. Korshin, R. Amal, Multi-wavelength spectroscopic and chromatography study on the photocatalytic oxidation of natural organic matter, Water Res. 44 (2010) 2525–2532.

[30] F.L. Palmer, B.R. Eggins, H.M. Coleman, The effect of operational parameters on the photocatalytic degradation of humic acid, J. Photochem. Photobiol., A 148 (2002) 137–143.

[31] F.J. Stevenson, Humus Chemistry: Genesis, Composition, Reactions, Wiley, New York, NY, 1982.

[32] A.W. Garrison, P. Schmitt, A. Kettrup, Capillary electrophoresis for the characterization of humic substances, Water Res. 29 (1995) 2149–2159.

[33] S. Van Geluwe, L. Braeken, B. Van der Bruggen, Ozone oxidation for the alleviation of membrane fouling by natural organic matter: A review, Water Res. 45 (2011) 3551–3570.

[34] J. Nawrocki, Comment on “outside-in trimming of humic substances during ozonation in a membrane contactor”, Environ. Sci. Technol. 41 (2007) 5161.

[35] R.H.S. Jansen, A. Zwijnenburg, W.G.J. van der Meer, M. Wessling, Outside-in trimming of humic substances during ozonation in a membrane contactor, Environ. Sci. Technol. 40 (2006) 6460–6465.

[36] D. Behar, G. Czapski, Itzhak Duchovny, Carbonate radical in flash photolysis and pulse radiolysis of aqueous carbonate solutions, J. Phys. Chem. 74 (1970) 2206–2210.

[37] J.L. Weeks, J. Rabani, The pulse radiolysis of deaerated aqueous carbonate solutions. I. Transient optical spectrum and mechanism. II. pK for OH radicals, J. Phys. Chem. 70 (1966) 2100–2106.

[38] H. Al-Ekabi, A. Safarzadeh-Amiri, W. Sifton, J. Story, Advanced technology for water purification by heterogeneous photocatalysis, Int. J. Environ. Pollut. 1 (1991) 125–136.

[39] M.G. Gonzalez, E. Oliveros, M. Worner, A.M. Braun, Vacuum-ultraviolet photolysis of aqueous reaction systems, J. Photochem. Photobiol., C 5 (2004) 225–246.

[40] G. Heit, A.M. Braun, VUV-photolysis of aqueous systems: Spatial differentiation between volumes of primary and secondary reactions, Water Sci. Technol. 35 (1997) 25–30.

[41] T. Tasaki, T. Wada, K. Fujimoto, S. Kai, K. Ohe, T. Oshima, Y. Baba, M. Kukizaki, Degradation of methyl orange using short-wavelength UV irradiation with oxygen microbubbles, J. Hazard. Mater. 162 (2009) 1103–1110.

[42] Y. Ku, L.S. Wang, Y.S. Shen, Decomposition of EDTA in aqueous solution by UV/H_2O_2 process, J. Hazard. Mater. 60 (1998) 41–55.

[43] D. Salari, A. Niaei, S. Aber, M.H. Rasoulifard, The photooxidative destruction of C.I. Basic Yellow 2 using UV/$S_2O_8^{2-}$ process in a rectangular continuous photoreactor, J. Hazard. Mater. 166 (2009) 61–66.

[44] E.R. Weiner, Applications of Environmental Chemistry, A Practical Guide for Environmental Professionals, Chapter 7, Lewis Publishers, CRC Press LLC, Boca Raton, FL, 2000.

[45] J. Méndez-Díaz, M. Sánchez-Polo, J. Rivera-Utrilla, S. Canonica, U. von Gunten, Advanced oxidation of the surfactant SDBS by means of hydroxyl and sulphate radicals, Chem. Eng. J. 163 (2010) 300–306.